International Journal of Science and Research (IJSR)
ISSN: 2319-7064
SJIF (2022): 7.942

Finite Element Analysis of Human Mandible and Development of Implant by Additive Manufacturing

Syed Abed Hashmi

Vasavi College Of Enegineering, Hyderabad, Telanga, India

Abstract: ***A computational study using DICOM (Digital Imaging and Communications in Medicine) information to create a 3D model of the jaw. The files were loaded into the Slicer 4D software, which was used to build the model by thresholding each slice of the file. The model was then imported as an STL file using the Siemens UG-NX 11.0 programme for convergent modelling, which transformed the facets into a single solid model. The model was imported into ANSYS-Workbench 2019R3 software with IGES file extension, with two different boundary conditions such as fixed supports and hinged supports on the condylar region of the jaw using Bone, Titanium (Ti6Al4V), PMMA, and PEEK as various materials, and Material optimization analysis was performed on the jaw. The behaviour of the implant was studied when the jaw was subjected to a mastication condition of 7.2MPa as the load as the maximum bite force and 0.5MPa as static pressure as the maximum pressure on the jaw, Suggesting the appropriate material for the implant from the analysis by comparing the results with the material properties of bone and the properties of different materials mentioned above, and 3D model is fabricated using STL file in Cura software and Ultimaker 3D as a machining platform.***

Keywords: DICOM images, convergent modeling, Finite Element Analysis, FDM

1. Introduction

The lower jaw is linked to the skull which is called as mandible. The lower teeth are supported by this bone, which is the largest and strongest in the facial skeleton. Mandibular defects are common in dental practise and can have a significant impact on masticatory performance.

The need for producing jaw implants arises from the fact that the jaw's connectivity is reduced as a result of bone fractures; previously, plates and screws were employed to protect the jaw's connections, but these plates and screws failed to maintain the jaw's strength. To address this, a new plating system was created utilising CAD/CAM/CAE to replace the jaw. To minimise time and effort during surgical operations, the U-shaped plate was devised based on the dimensions of the genuine human jaw. [1] To examine the stresses and reaction forces during normal sagittal closure, a 2D finite element model of the human temporomandibular joint was created. This was done in two stages. The first was used to calculate condylar displacements, and the second was used to calculate mechanical parameters using a finite element model [2]. The procedure for obtaining a bio-CAD model of the mandible from computed tomography (CT), 2D segmentation, calculating a 3D object from scanned data, reverse engineering interface, point cloud data processing, surface reconstruction, solid model reconstruction, obtaining a bio-CAD model, and fabricating the model using RP technology were all investigated in this study [8]. Many strategies have been used to reconstruct mandibular designs, but those designs do not match the expectations of patients, as the mandible is a movable bole that folds the skull and articulates with it through teeth. The horizontal bars, curved part, and curved part were used to resemble a space frame model and two load instances were investigated: one with symmetrical loading and the other with a load of 100N on the left side, as well as the material properties of the bone and PMMA [12].

2. Methodology

2.1 Problem Identification

Implants in the mandible are extremely particular in usage, due to the discovery of tumours in the bone, cracks, or fractures in the jaw. They may be common due to the formation of cavities in the teeth root area in the jaw or due to accidents, according to research. [3]. As a result, there was a need to improve the quality of implants or the design of implants; current improvements in implants, such as plates and screws, have failed to maintain the strength of the jaw with several fractures. Biomodelling of the jaw can be used as an input for analysis and production to solve the challenges of building a complicated structure. The workflow and the process methodology is carried out to develop the prototype model of the jaw is as shown in fig 1.

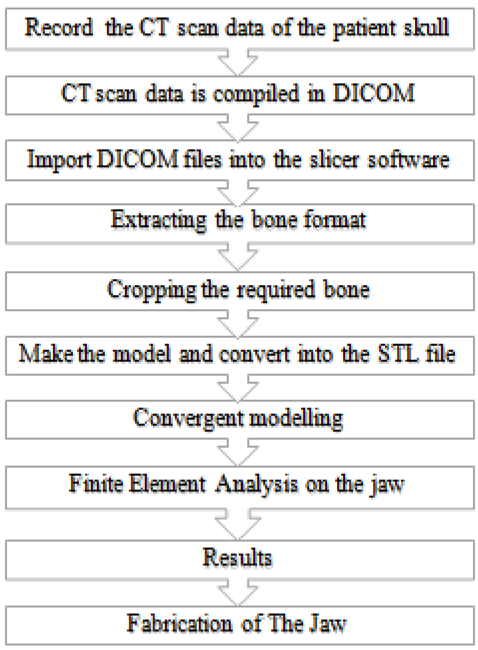

Figure 1: Workflow of patient-specific jaw analysis.

Anatomical modelling refers to models of a patient's anatomical data that were created using CT scan data from the Digital Imaging and Communication in Medicine (DICOM) file. Using medical files to create a 3D model. The CT scan head section of a 65-year-old male patient is sent to the doctor in DICOM format, which must be imported into the Slicer 3D software's volume module, as illustrated in Fig 2.

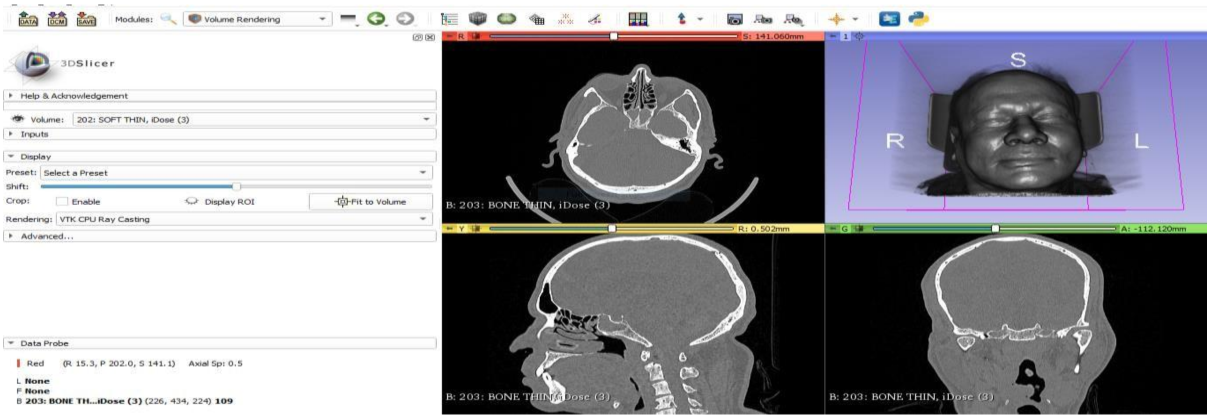

Figure 2: Showing the DICOM file imported in the volume module of the slicer software

The next step is to use the Slicer programme to retrieve the CT scan data from the bone formation. This is accomplished by switching the session to CT bone and shifting the form to need, as illustrated in Fig 3.

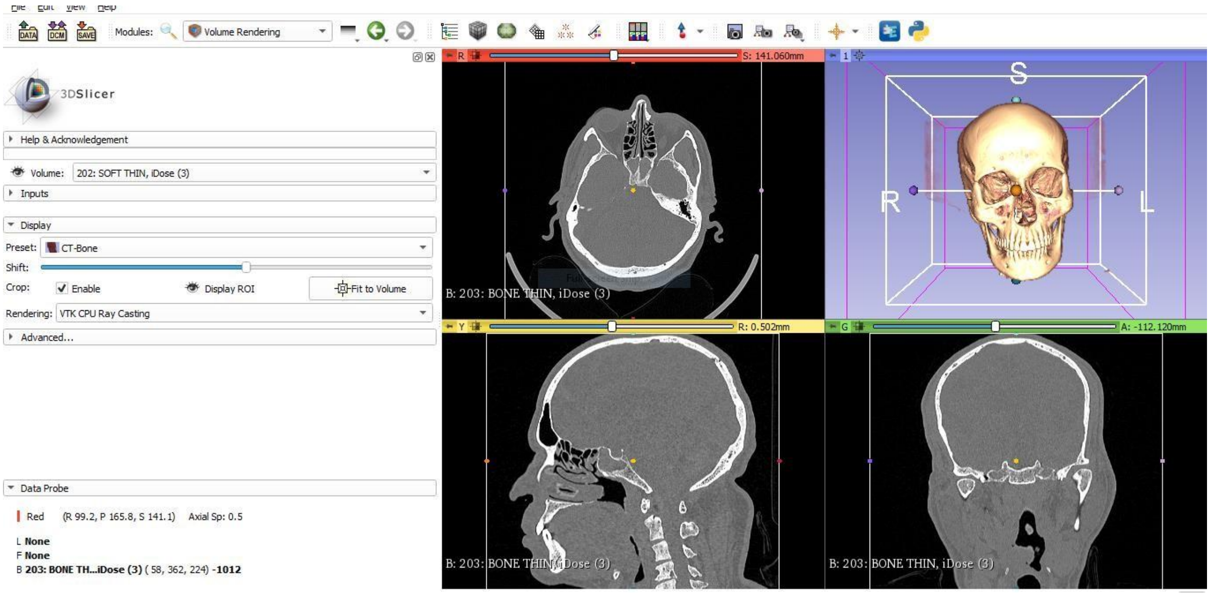

Figure 3: Extraction of the CT- Bone part from the DICOM file

We attempted cropping the required section but didn't get the only required part for this, therefore we have to threshold the part of the mandible using the thresholded, as we only require the lower jaw. To acquire good results in the analysis, thresholding must be done carefully, since it may result in low-quality parts in the solution of the problem. After the chopped and only required session has been thresholded, the model is created using the model creating option in the editing module, as illustrated in Fig 4 (a) and Fig 4 (b).

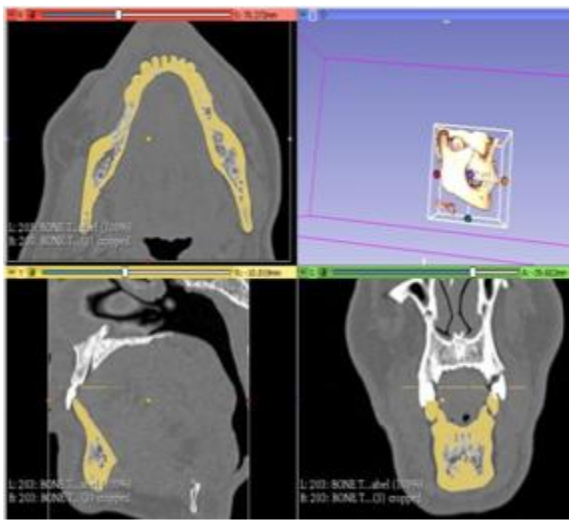

Figure 4 (a): Thresholding using paint option to make the required model

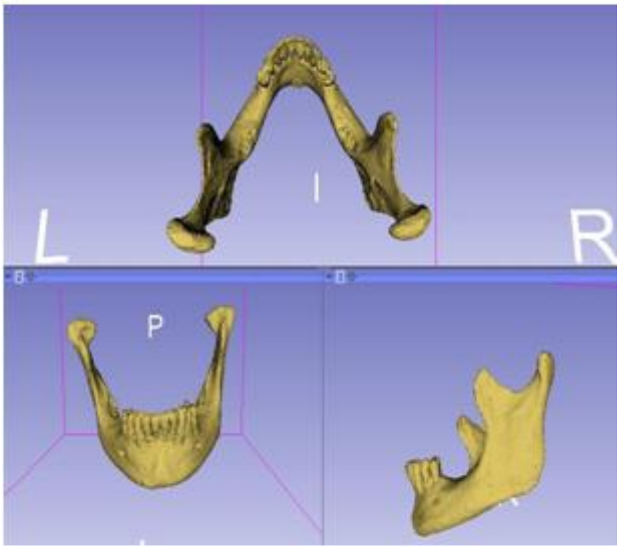

Figure 4 (b): different views of mandible model made in the slicer software

2.2 Convergent Modelling

After the model has been created, it is saved in the STL (stereolithography) file format in order to move on to the next processes, which include convergent modelling, Finite element analysis, and fabrication. Convergent modelling gets its name from the fact that it combines meshes and solids into a single model. Convergent modelling is intended to provide three major advantages to designers:

1) Improve part design for 3D printing
2) Make the whole design process go faster
3) Make reverse engineering in product design a more common and efficient process.

We must import the model in the STL file format into the NX 11 software to converge the facets, meshes, and solids into a single model for convergent modelling; therefore, we can convert the files by selecting the menu option in the required format.

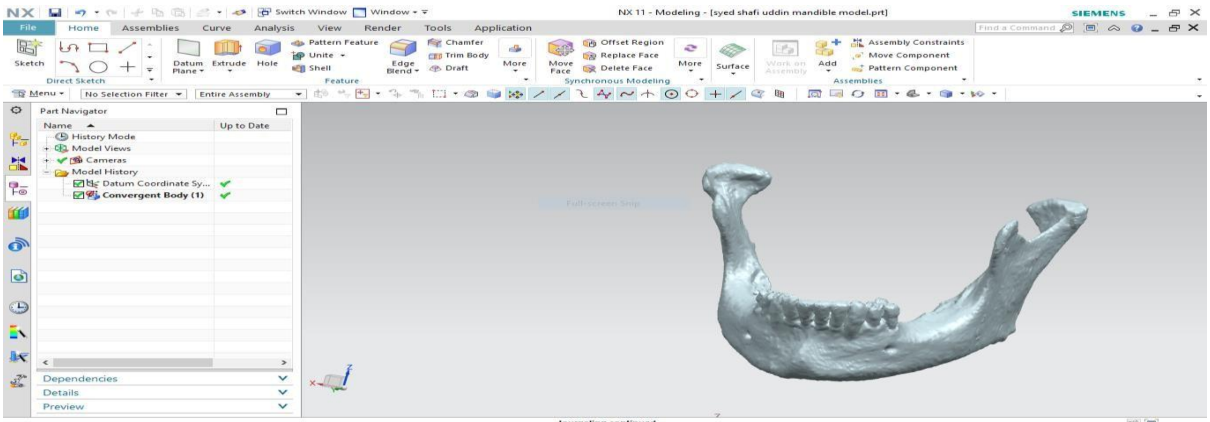

Figure 5: Convergent modeling of the lower jaw in the NX software

After creating the convergent model in the NX 11.0 programme, as illustrated in Fig 5, the model is ready for further processing such as analysis and 3D printing.

2. Materials to be used in the project's implants the following materials were used for the implants:

- Titanium Alloy is a metal alloy made of titanium (Ti6AL4V)
- PMMA (Polymethylmethacrylate) (Poly Methyl Methacrylate)
- PEEK (Poly Etherether Ketone)
- Bone

The materials chosen for the implants are listed in table 1 along with their material parameters such as Youngs modulus, possion's ratio, density, tensile yield strength, and ultimate tensile strength.

Table 1: Material properties for the mandible implants

	Biomaterials Selected			
Properties	(Ti6Al4V)	(PMMA)	(PEEK)	BONE
Young's Modulus (MPa)	110000	3000	4000	3000
Poisson's ratio	0.3	0.38	0.4	0.3
Ultimate tensile strength (MPa)	950	72	103	150
Yield strength (MPa)	800	72	100	100
Density(kg/mm^3)	4.43E-06	1.18E-06	1.36E-06	1.85E-06

2.3 FEA on the convergent model of the jaw

Static structural analysis allows us to predict the effects of steady loading conditions on the structure and investigate the changes in the structure under various boundary conditions and loads. The interface for static structural analysis in ANSYS WORKBENCH 2019 R3 Import the IGES-formatted mandible file into the geometry module of the static structural analysis. The imported mandible is meshed with a tetrahedral mesh using the patch conforming method, with a global element size of 2mm (see Fig 7).

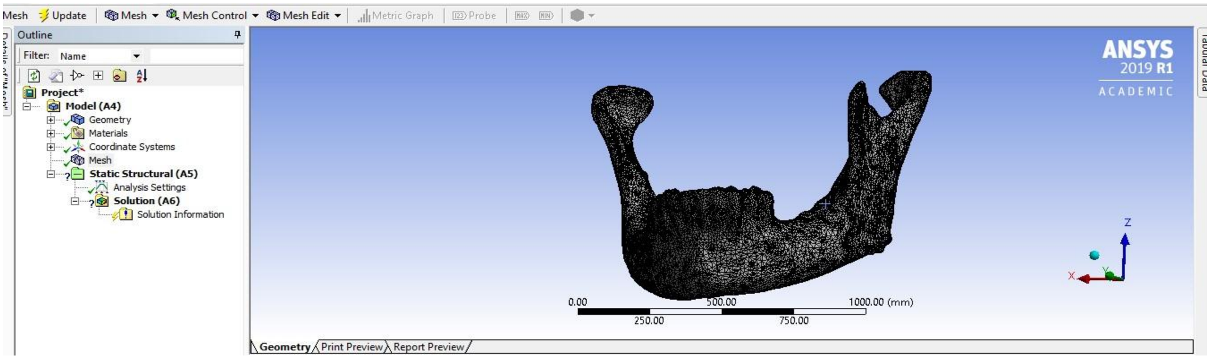

Figure 7: Tetrahedral meshing of the mandible with element size 2mm

On the condylar region of the mandible, the analysis includes two different boundary conditions: hinged boundary condition and fixed boundary condition. To put the boundary conditions in place. We must define loads in the pre-processor under which displacement is picked, which results in two cases of analysis for the project.

1) End condition on the condylar section is fixed - (select All DOF)
2) The condylar component has a hinged end condition – (select only Fx and Fz)

Select the needed nodes for the application of load on the jaw for the following two loading conditions: For the application of load on the jaw select the required nodes for two loading conditions they are as follows:

1) Point load as the maximum force required to bite i.e., 7.2MPa
2) Uniformly distributed pressure Load on the jaw i.e., 0.5MPa, as the muscle force on the jaw during mastication condition.

For the static structural study in ANSYS- Workbench 2019R3 with fixed and hinged supports, the boundary conditions and load applications on the jaw necessary for mastication are presented in Figure. 5.5 and 5.6, respectively.

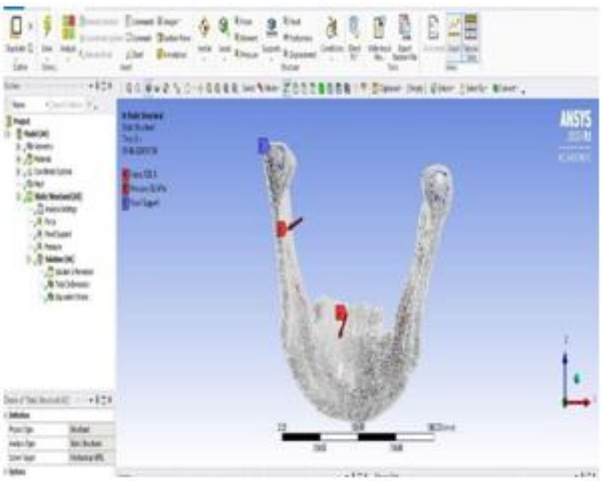

Figure 8 (a): Fixed end Boundary conditions and load application on the jaw during mastication

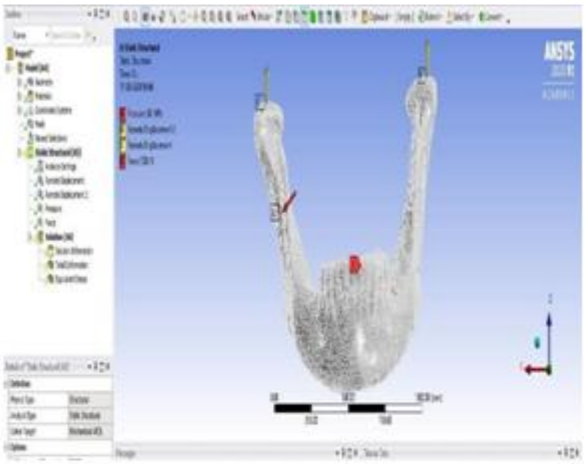

Figure 8 (b): Hinged end Boundary conditions and load application on the jaw during mastication

2.4 Manufacturing the Jaw Using Fused Deposited Machining

Fused Deposited Machining is used to create the jaw while not every 3D printer can meet the level of expectations, a few can. 3D printing has provided numerous opportunities to develop intricate and complex parts, whether in the medical field or aerospace. Specialized industries have dedicated to achieving the highest precision and accuracy, and while not every 3D printer can match the level of expectations, a few can. One such machine is the Ultimaker 3 Extended, which is depicted in Figure 9.

Figure 9: Showing the machine Ultimaker 3 Extended

The strength of the model to be created is defined by this infill pattern. The pattern is determined by the density of the infill, which defines the air gap between the geometry. The greater the density, the greater the model's strength. In order to manufacture the complex structure, patterns must be assigned and support must be provided. The Ultimaker Cura software is used, which allows us to import geometry in STL file format, as shown in fig 10.

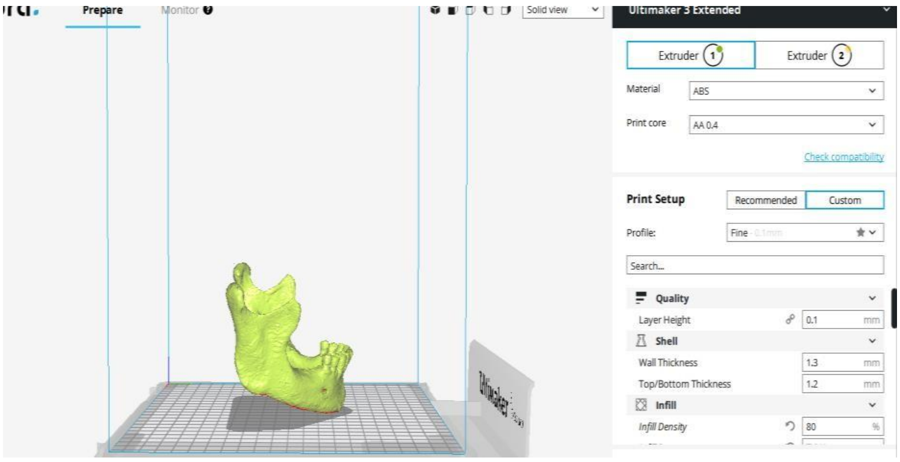

Figure 10: **S**howing the jaw imported in the CURA software

The G-code programme is generated in Cura software to manufacture the jaw, and this code is stored in the drive, and setup is opened in a machine that estimates the time required for building the model in the machine, and printing begins, as shown in Fig 11.

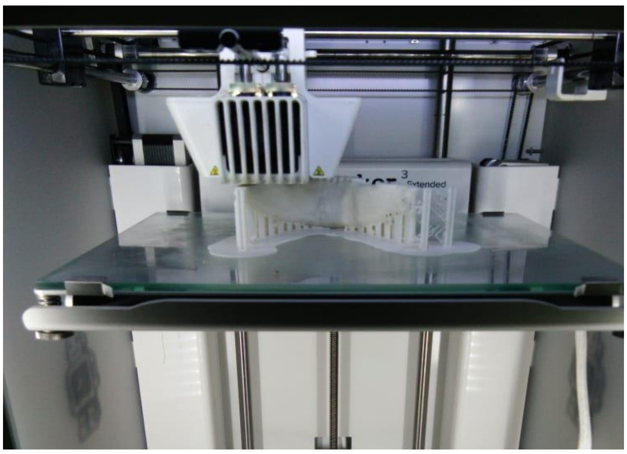

Figure 11: Printing the jaw prototype in Ultimaker 3D extended

As the prototypic implant is manufactured using the STL file model created in the medical software slicer, it took about 1 day, 22 hours to create the jaw and the fine model of the jaw. The finished model is shown in Fig 12 after it has been completely manufactured.

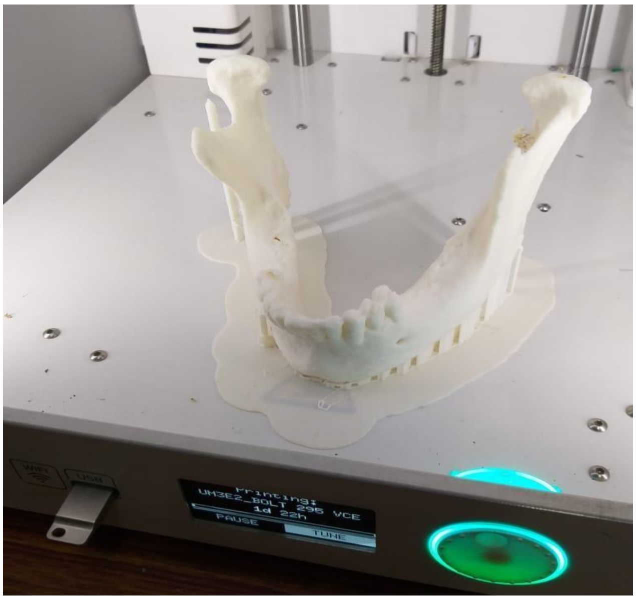

Figure 12: (3D printed prototypic jaw)

3. Results

The implant materials were taken into the study, and analysis was performed on the jaw with different implant material, which suits the best alternative for the jaw implants were Titanium Alloy, PMMA, and PEEK, according to the work specified analysis and development of mandible implants. The analytical results are summarised by depicting the various materials and their total deformation values, as well as the Equivalent von Mises stress values. The static structural analysis performed on the lower jaw in Ansys Workbench 2019 R3 yielded the results deformation values and maximum and minimum equivalent stress of two cases solved in ANSYS- Workbench 2019 R3. Maximum deformation values for fixed end conditions are 8.7314mm for bone, 20.273mm for PMMA, 15.178mm for PEEK, and 5.5563mm for Ti-alloy. While the Equivalent Von Mises stresses are 0.0007 and 30.18MPa for bone, 0.0007 and 28.15MPa for PMMA, 0.00068 and 27.59MPa for PEEK, and 0.0007 and 30.18MPa for Titanium Alloy, respectively. Graph 1 depicts the variation of deformation and equivalent stress for different materials under the same load but with fixed supports.

The minimum and maximum deformation values for hinged end conditions are 0.00692 and 6.064mm for bone, 0.00169 and 14.243mm for PMMA, 0.0128 and 10.697mm for PEEK, and 0.00044 and 0.3859mm for Ti-alloy, respectively, While the Equivalent Von Mises stresses are 0.00018 and 15.97 MPa for Bone, 0.00013 and 16.49 MPa for PMMA, 0.00018 and 16.65 MPa for PEEK, and 0.00018 and 15.97 MPa for Titanium Alloy, respectively. Graph 2 depicts the variation of deformation and equivalent stress for different materials under the same load but with hinged supports.

Table 2: Static structural analysis results of the jaw with different materials

Material	Boundary condition	Total deformation (mm)		Equivalent stress (Von-Mises) (MPa)	
		Min	Max	Min	Max
BONE	Fixed End	0	8.7314	0.00070	30.18
PMMA	Fixed End	0	20.273	0.00070	28.15
PEEK	Fixed End	0	15.178	0.00068	27.59
Ti -ALLOY	Fixed End	0	5.5563	0.00070	30.18
BONE	Hinged End	0.00692	6.064	0.000181	15.97
PMMA	Hinged End	0.01693	14.243	0.00013	16.492
PEEK	Hinged End	0.01286	10.697	0.000189	16.554
Ti- ALLOY	Hinged End	0.000440	0.3859	0.000181	15.972

In this analysis the deformation and stress on the jaw helps us to estimate out the implant material suitable for the bone, following fig 13 (a) and 13(b) shows the total deformation and the equivalent von mises stress on the jaw with **BONE** material properties under **fixed** conditions on the condylar region respectively.

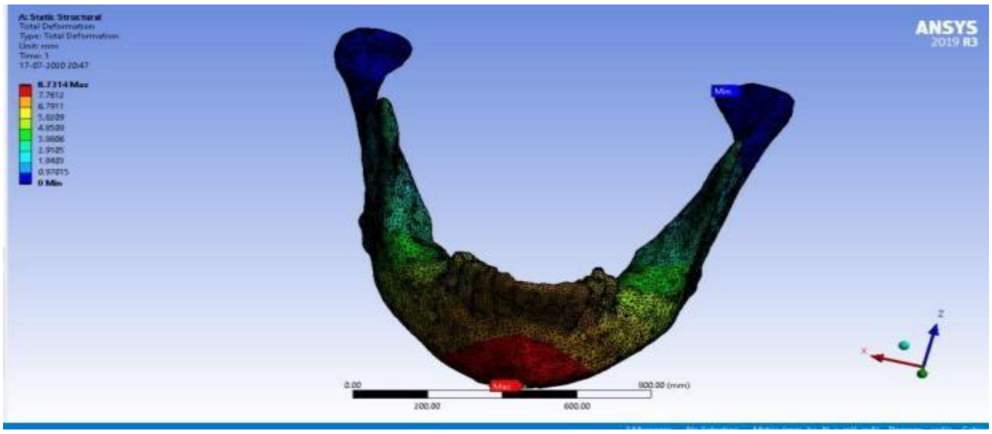

Figure 13 (a): Total deformation of the jaw, fixed condition for bone

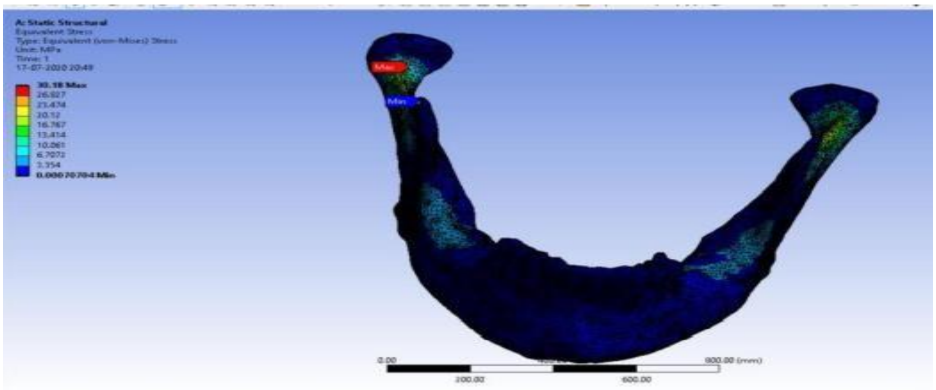

Figure 13 (b): Element stress (Von-Mises) of the jaw, fixed condition for bone

The following fig 14(a) and 14(b) shows the total deformation and the equivalent von mises stress on the jaw with **PMMA** material properties under **fixed** conditions.

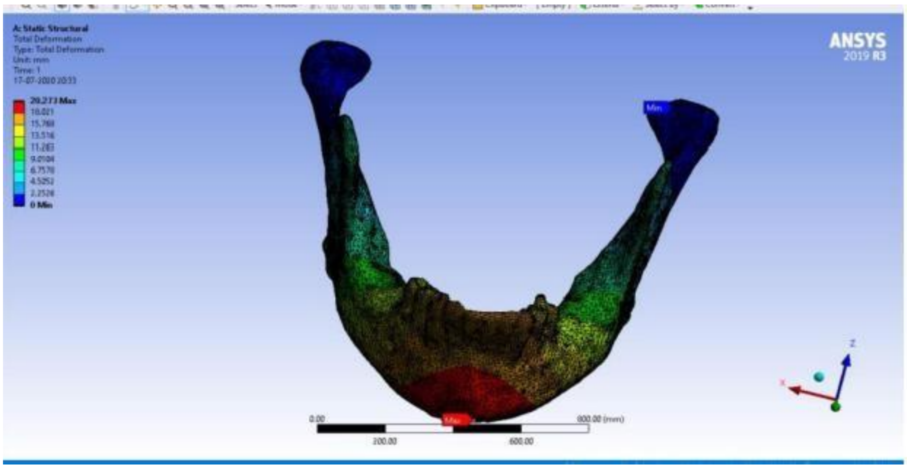

Figure 14 (a): Total deformation of the jaw fixed condition forPMMA

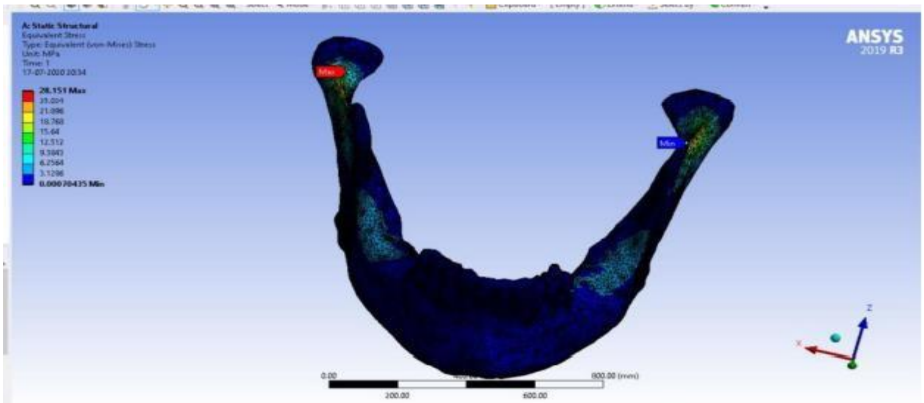

Figure 14 (b): Element stress (Von-Mises) of the jaw, fixed condition forPMMA

The following fig 15(a) and 15 (b) shows the total deformation and the equivalent von mises stress on the jaw with **PEEK** material properties under **fixed** conditions.

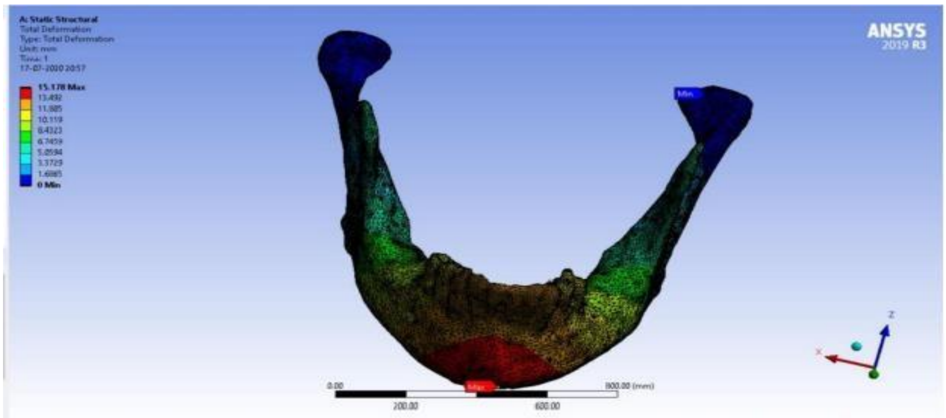

Figure 15 (a): Total deformation of the jaw, fixed condition for PEEK

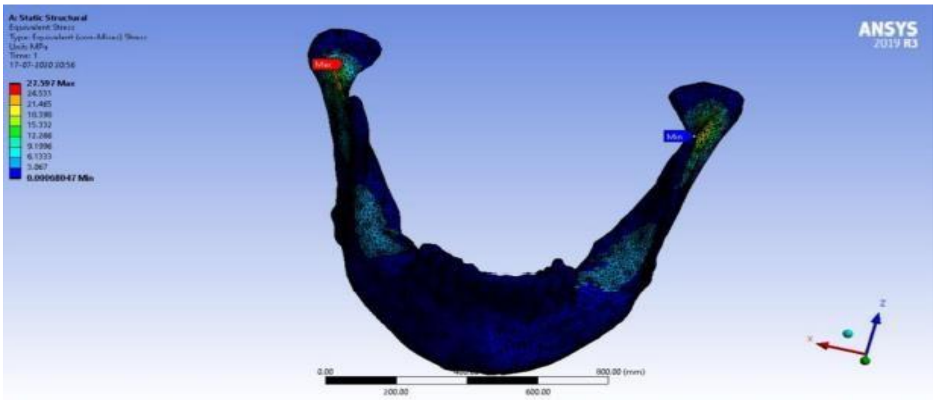

Figure 15 (b): Element stress (Von-Mises) of the jaw, fixed condition for PEEK

The following fig 16(a) and 16 (b) shows the total deformation and the equivalent von mises stress on the jaw with **Titanium Alloy** properties material properties under **fixed** conditions on the condylar region respectively.

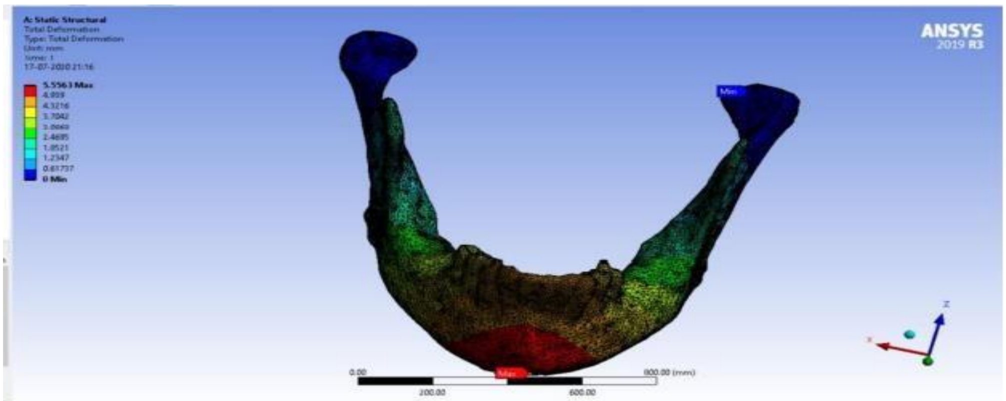

Figure 16 (a): Total deformation of the jaw, fixed condition for Titanium-Alloy

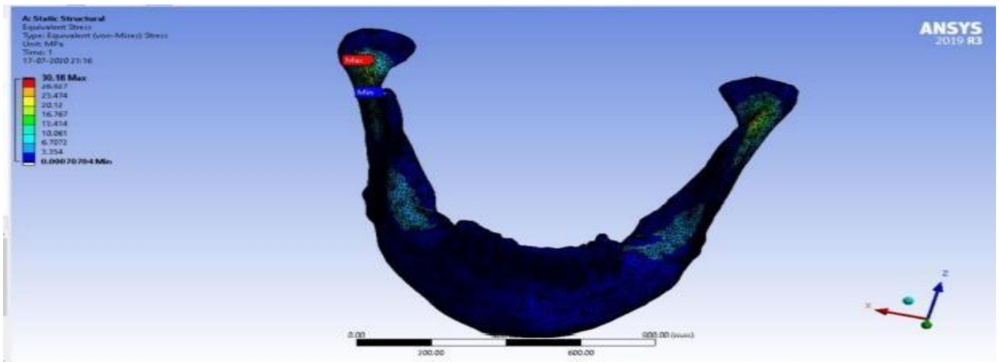

Figure 16 (b): Element stress (Von-Mises) of the jaw fixed condition for Titanium- Alloy

International Journal of Science and Research (IJSR)
ISSN: 2319-7064
SJIF (2022): 7.942

The following fig 17(a) and 17(b) shows the total deformation and the equivalent von mises stress on the jaw with **BONE** material properties under **Hinged** conditions on the condylar region respectively.

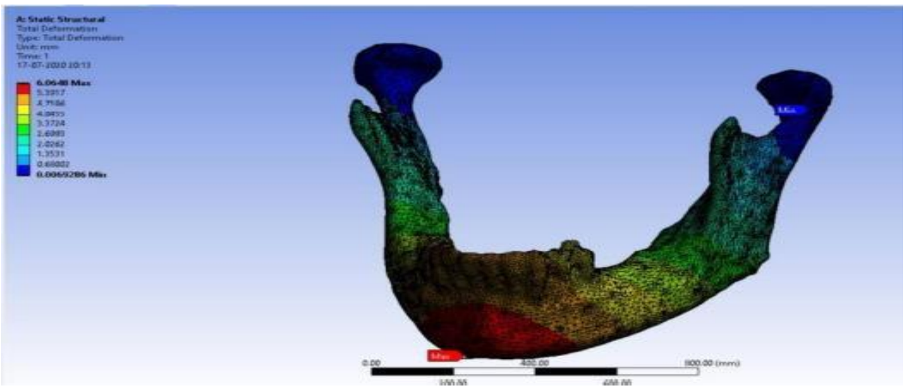

Figure 17 (a): Total deformation of the jaw Hinged condition for Bone

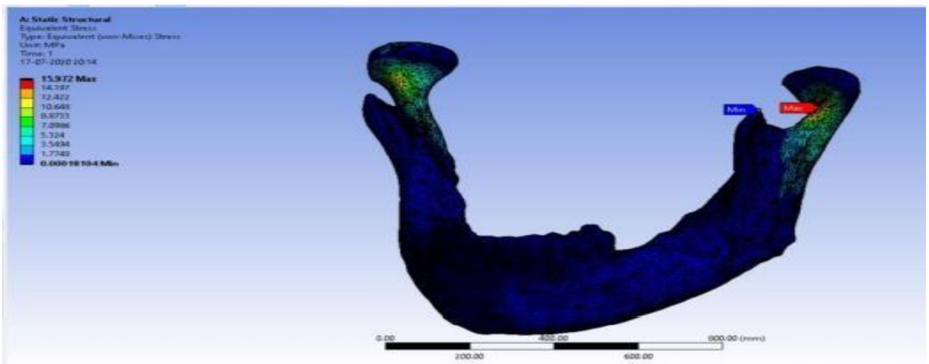

Figure 17 (b): element stress (Von-Mises) of the jaw, Hinged condition for Bone

The following fig 18(a) and 18(b) shows the total deformation and the equivalent von mises stress on the jaw with **PMMA** material properties under **Hinged** conditions on the condylar region respectively.

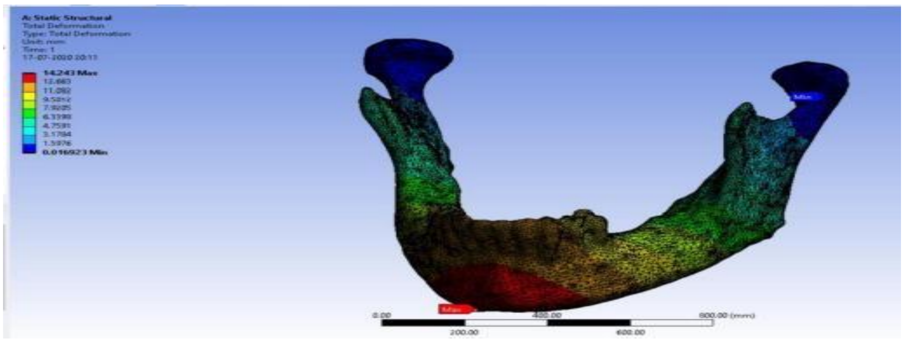

Figure 18 (a): Total deformation of the jaw, Hinged condition for PMMA

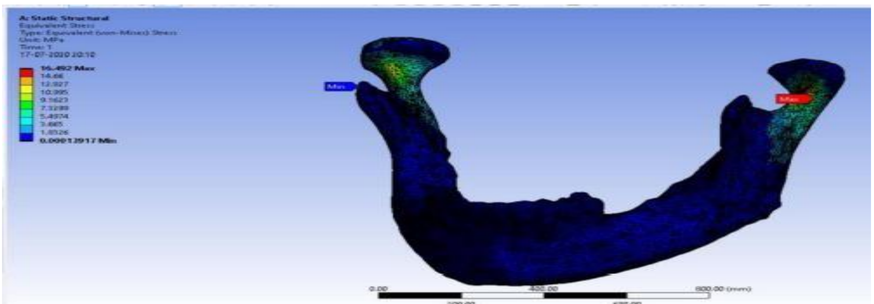

Figure 18 (b): Element stress (Von-Mises) of the jaw, Hinged condition for PMMA

The following fig 19(a) and 19(b) shows the total deformation and the equivalent von mises stress on the jaw with **PEEK** material properties under **Hinged** conditions on the condylar region respectively.

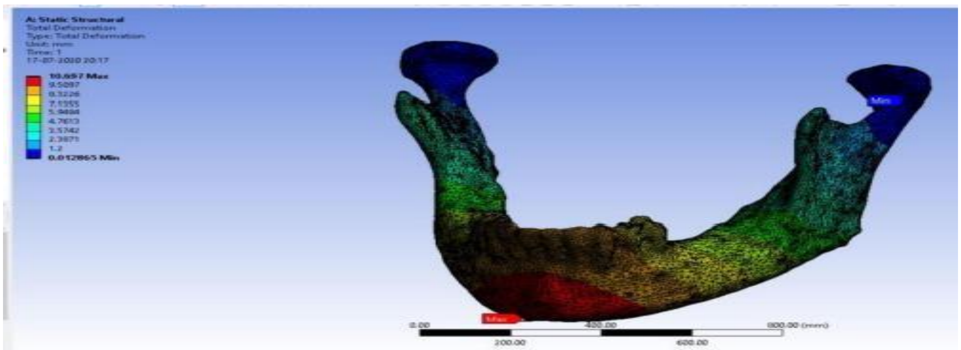

Figure 19 (a): Total deformation of the jaw, Hinged condition for PEEK

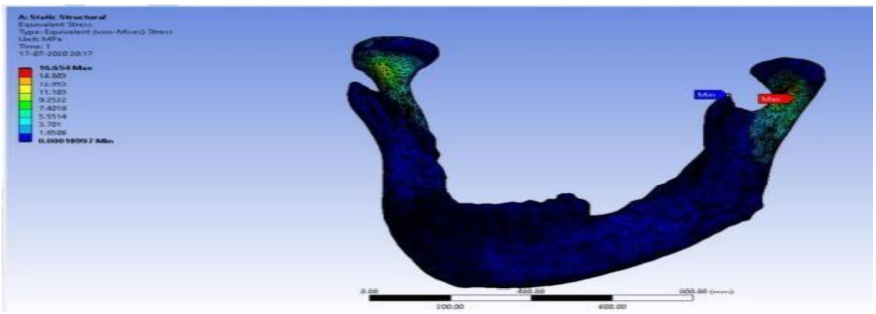

Figure 20 (b): Element stress (Von-Mises) of the jaw, Hinged condition for PEEK

The following fig 20(a) and 20 (b) shows the total deformation and the equivalent von mises stress on the jaw with **Titanium Alloy** material properties under

Hinged conditions on the condylar region respectively

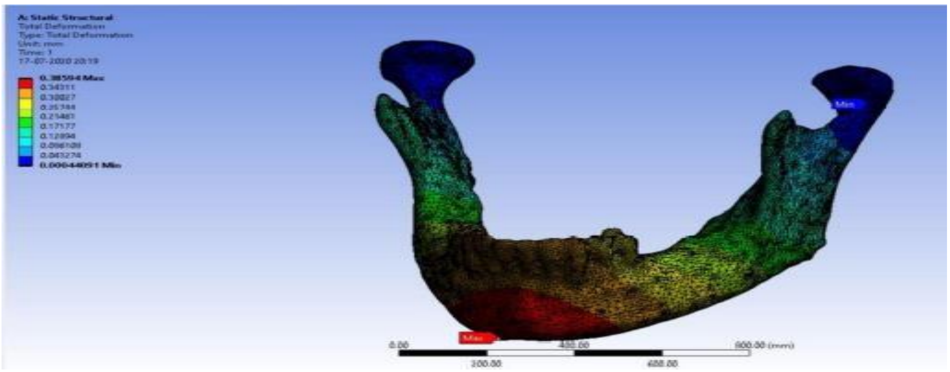

Figure 20 (a): Total deformation of the jaw, Hinged condition for Titanium-Alloy

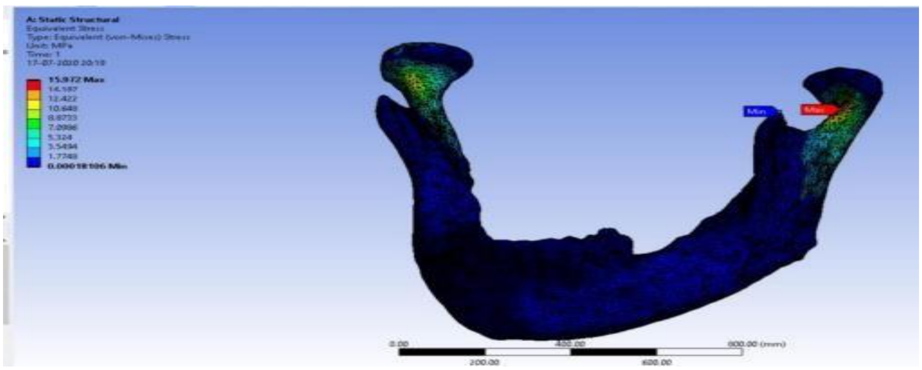

Figure 20 (b): element stress (Von- Mises) of the jaw, with Hinged condition for Titanium-Alloy

The variation of deformation and equivalent stress for different material with same load but with fixed supports is plotted in graph 1. The variation of deformation and equivalent stress for different material with same load but with Hinged supports is plotted in graph 2.

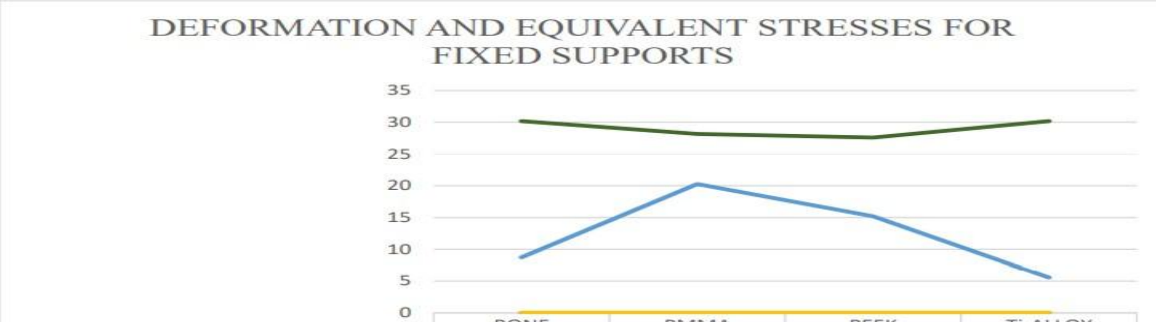

	BONE	PMMA	PEEK	Ti-ALLOY
MIN DEFORMATION (mm)	0	0	0	0
MAX DEFORMATION (mm)	8.7314	20.273	15.178	5.5563
MIN EQVIVALENT STRESS (MPa)	0.0007	0.0007	0.00068	0.0007
MAX EQUIVALENT STRESS (MPa)	30.18	28.15	27.59	30.18

Graph 1: Deformation and Equivalent stress for different materials under fixed end conditions

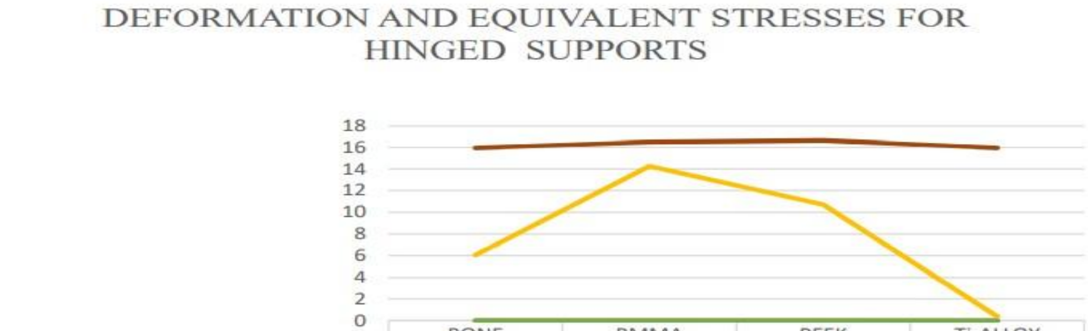

	BONE	PMMA	PEEK	Ti-ALLOY
MIN DEFORMATION (mm)	0.00692	0.0169	0.0128	0.0004
MAX DEFROMATION (mm)	6.064	14.243	10.697	0.3859
MIN EQUIVALENT STRESS (MPa)	0.00018	0.00013	0.00018	0.00018
MAX EQUIVALENT STRESS (MPa)	15.97	16.49	16.65	15.97

Graph 2: Deformation and Equivalent stress for different materials under Hinged end conditions

4. Conclusion and Discussion

The following conclusions can be derived from the detailed thesis report

The detailed report leads to the following conclusions.

Procedures can be completed successfully with the use of 3D printing technology. The production of MRP (medical rapid prototype) models using 3D printing provides low-cost anatomical models that are useful in surgical planning. This fabrication reduces the time required for surgical procedures to correct the problem, and it will be of great assistance to dentists in understanding the anatomy of mandibular defects. 3D printing allows for real-time practise of surgery on a prototype that closely resembles the actual body part structure. Using Ansys Workbench2019R3, a static structural analysis of the mandible was performed with input data of various biocompatible materials under two boundary conditions The maximum deformation on the jaw with bone properties was found to be 8.7314 mm under fixed end conditions and 6.064 mm under hinged conditions, with equivalent stress (Von-Mises) values of 0.0007 MPa min and 30.18 MPa max for fixed end and 0.00018 MPa min and 15.97 MPa max for hinged conditions. The deformation on the jaw for the alternate material was found to be 15.178 mm under fixed end condition and 10.697 mm under hinged condition and Equivalent stress (Von-Mises) were 0.00068 MPa min and 27.59 MPa max for fixed end and 0.00018 MPa min and 16.65 MPa max for hinged condition. Titanium alloy has the necessary properties to replace bone, but its high cost makes it unaffordable. The next alternative material for bone implants is PEEK, which is less expensive and nearly matches the values of bone.

References

[1] A.T. Abbas. CAD/CAM/CAE reconstruction skeleton for the lower human jaw (2011)

[2] A clinical and technical overview of fabricating CAD/CAM implant-retained mandibular bar overdentures. Chui Ling Goo1 and Keson Beng Choon Tan2 (2017)

[3] Biomechanical stresses and strain analysis of the human mandibular region from computer tomography to custom implant development. Rafael Ferreira Gregolin, Cecilia Amelia de Carvalho Zavaglia, Rus Camargo Tokimatsu, and Joo A. Pereira are the authors. (2017)

[4] 3D customised models of the human mandible are designed and analysed. Massimo Martorelli, Saverio Maietta, Antonio Gloria, Roberto De Santis, and Eujjin Pei are among the cast members (2015)

[5] Mandibular geometric parameters in 3D CBCT imaging Wojciech Ryniewicz, Anna Ryniewicz, Lukasz Bojko

[6] Patient-specific cranial implants are created using finite element analysis and additive manufacturing. G. Pradeep Vasavi Engineering College (2018)
[7] Finite element analysis was used to predict the location of a failure in an additively manufactured mandible implant. Per Derand, Lars-Eril Rannar, Jan Micheal, E.Kristofer-Gamstedt, Jinxing Huo (2015).
[8] Rapid prototyping technology for 3D bio-cad modelling of the human mandible. Mustafa Aya, Tinaz Kubatb, Cagri Delilbasic, Bulent Ekicid, Huseyin Emir Yuzbasioglue, and Selim Hartomacioglu are among the players. (2013).
[9] An Investigation of Two Finite Element Modeling Solutions for Biomechanical Simulation Using a Case Study of a Mandibular Bone DECEMBER 2017, Vol. 139 / 12100
[10] Thesis work on modelling and fabrication of a 3D printed prototype model of the lumbar spine for study and training in endoscopic surgery. Dr.L. Siva Rama Krishna Vidyasagar Associate Professor Osmania University.
[11] 3D finite element simulation of the mandibular opening movement in healthy and pathologic simulations.
[12] Parametric modelling of the human mandible lateral body for section shape optimization during bone augmentation.Mircea Suciu, Razvan Cazacu, and Bica Cristina Ioana (2014).
[13] Mandibular prosthesis design and finite element analysis M. Anbuurjan, P U Ilavarasi, SRM University, Tamil Nadu (2011)
[14] Theoretical prediction of mandibular muscle forces during a bite, D.P. Updike, Q.S. Kang, and Eric P. Salathe (1990)
[15] The unique design of a patient's 3D printed whole mandible implant. Ian Gibson, Angus P. Fitz Patrick, and Mazher I Mohammed (2017)